



学 位 論 文

Correlation between transcranial Doppler ultrasonography
and regional cerebral blood flow in experimental
intracranial hypertension

Stroke, in press, 1997

永 井 秀 政

Correlation Between Transcranial Doppler Ultrasonography and Regional Cerebral Blood Flow in Experimental Intracranial Hypertension

Hidemasa Nagai, MD; Kouzo Moritake, MD, PhD; Mikio Takaya, MD, PhD
Department of Neurosurgery, Shimane Medical University

Background and Purpose Transcranial Doppler ultrasonography (TCD) provides useful information on cerebral circulation even under raised intracranial pressure. This study was designed to evaluate the correlation between cerebral blood flow (CBF) and TCD parameters under conditions of boundary intracranial hypertension that can cause brain death.

Methods Intracranial pressure was raised by inflation of a supratentorial epidural balloon in cats. Blood flow velocity of the middle cerebral artery was measured transorbitally with microvascular Doppler sonography, and intracranial pressure and CBF were evaluated.

Results In this study, four characteristic flow patterns were observed, appearing in the following order with progressive increases in intracranial pressure: sharp wave, systolic flow, systolic spike, and no flow. These flow patterns showed a significant correlation with flow velocity, CBF, the pulsatility index, and cerebral perfusion pressure. The systolic spike and no flow patterns and pulsatility index over 4.0 indicated decreased CBF, under 10% of control values.

Conclusions The critical level of brain circulation can be detected by Doppler sonography, indicating that TCD is available as a tool for the assessment of cerebral circulatory arrest in brain death.

(Stroke, in press, 1997)

Key Words · brain death · cerebral blood flow · intracranial pressure · ultrasonics · cats

Address reprint requests to: H. Nagai, MD,
Department of Neurosurgery, Shimane Medical University,
Enya-cho 89-1, Izumo, Shimane 693, Japan.
E mail address: nogeka@shimane-med.ac.jp

Several methods for measuring CBF have been designed to confirm the diagnosis of brain death in a person who meets the basic criteria of apnea, unresponsivity, and absence of all cephalic reflexes. Conventional cerebral angiography, digital subtraction angiography, dynamic CT, and radionuclide scanning provide final proof of absence of cephalic function. Such supplemental examinations may be expensive, invasive, and technology intensive and usually require transportation of the critically ill patient.

TCD enables us to measure the blood flow velocity in intracranial vessels repeatedly. Characteristic flow patterns in relation to ICP have been demonstrated, raising the possibility of monitoring increased ICP noninvasively. Several authors^{1,2} have attempted to adopt TCD for the evaluation of brain death and to establish Doppler ultrasound criteria for the diagnosis of brain death. Petty et al³ have reported that the flow patterns indicating either absent or reversed diastolic flow or small early systolic spikes showed high specificity and sensitivity in the detection of brain death. Unfortunately, these reports have not been backed up by the CBF data.

In this study, we investigated whether TCD parameters were correlated with ICP and CBF even under extreme intracranial hypertension.

Materials and Methods

Intracranial Hypertension Model

This experimental protocol was approved by our animal care use committee (Guidelines for Animal Experiments of the Shimane Medical University, March 1, 1990). Five mongrel adult cats of both sexes, weighing 3.0 to 5.5 kg, were anesthetized with pentobarbital (20 mg/kg IP) and tracheotomized. The femoral artery and vein were cannulated for the monitoring of systemic blood pressure and for drug injection. Animals were paralyzed with pancuronium bromide (0.1 mg/kg IV), and mechanically ventilated with a Harvard pump (model 613, Harvard Apparatus Co). The tidal volume and respiratory rate of the ventilator were controlled to maintain a PaCO₂ of approximately 40 mm Hg. The animals were placed in the prone position in a stereotactic frame (Tokyo Medical). A burr hole was made in the right parietal region and used to insert a latex balloon into the epidural space. The balloon was inflated at a rate of 0.047 mL/min using a microinfuser (Turusu A-2, Nakagawa-Seikodo) to elevate ICP.⁴ A fiberoptic microtransducer (Camino Digital Pressure Monitor 420, Camino Laboratories) was inserted through another burr hole into the left parietal epidural space for measurement of ICP.

Measurement of CBF

Regional CBF of the ectosylvian gyrus of cats was measured transdurally, using a laser-Doppler flowmeter (laserflo BPM403, TSI Inc), through a burr hole. The burr hole was carefully opened to avoid the leakage of cerebrospinal fluid and was sealed with methyl methacrylate (Toughron Rebase, Miki Chemical Products Co, Ltd) after the insertion of monitoring probes (Fig 1). To exclude any artifacts due to respiratory movement and brain pulsation in the statistical analysis, we calculated a value termed "percent CBF" (pCBF), which is defined as follows: $pCBF = (CBF - bgCBF) / (blCBF - bgCBF) \times 100 (\%)$. Baseline CBF (blCBF) was measured before balloon inflation, and background CBF (bgCBF) was measured at the time of cardiac arrest in each animal.

Measurement of TCD Parameters of the MCA

The MCA was carefully approached using the transorbital procedure,⁵ avoiding dural tears and cerebrospinal fluid leakage. Blood flow in the MCA could be easily measured transdurally with the Doppler flowmeter.⁶

To correlate the Doppler waveform with CBF, we recorded serial TCD parameters, blood pressure, and ICP every 5 minutes during inflation of the epidural balloon. The TCD parameters consisted of peak systolic flow velocity (V_s), end-diastolic flow velocity (V_{ed}), and mean flow velocity (MFV). The mean flow velocity was calculated as the time-averaged value of the envelope of the Doppler sonogram. Dimensionless variables such as the PI⁷ and RI⁸ are not dependent on the insonation angle and were calculated for each flow velocity. PI and RI were calculated as $PI = (V_s - V_{ed}) / MFV$ and $RI = (V_s - V_{ed}) / V_s$, respectively. These parameters were considered to indicate the peripheral vascular resistance.

Electroencephalography

To evaluate microcirculatory thresholds for the electrical activity of the cerebral cortex, ECoG was recorded using an electroencephalograph (EEG-7209, Nihon Kohden) with the silver electrode placed over the left ectosylvian gyrus.

Statistical Analysis

The data were analyzed statistically by ANOVA and calculation of Spearman's rank correlation coefficients. Correlation of parameters was calculated by a single linear regression.

Results

Relationship Between Flow Patterns, ICP, and CBF

Doppler sonograms obtained in this model of progressive intracranial hypertension

showed four characteristic flow patterns in the following sequence (Fig 2). (1)SW: A progressive increase in ICP brings about a more rapid reduction in flow velocity in the diastolic phase than in the systolic phase, resulting in pronounced pulsatility between peak systole and end of diastole. This flow pattern is referred to as the "sharp wave". (2)SF: Following a further rise in ICP, the diastolic part of the flow velocity spectrum starts to disappear. This was referred to as the "systolic flow" pattern. (3)SS: Further elevation of ICP diminishes the waveform, resulting in a brief peak in systole called the "systolic spike". (4)NF: At the final stage of intracranial hypertension, Doppler signals were not detected at all, and this is termed "no flow".

Sequential changes in mean flow velocity, RI, PI, ICP, blood pressure, CPP, and CBF at every stage of the Doppler flow pattern are shown in the Table. With increases in ICP, RI and PI increased and mean flow velocity decreased in all animals. The mean values of these variables showed significant rank correlation ($p < .001$, Spearman's test). On the basis of these data, CPP under raised ICP could be defined as the difference between blood pressure and ICP. Since ICP was increased by inflation of the epidural balloon, it had the potential to surpass blood pressure. Negative CPP reflects such a critical condition.

Correlation Between TCD Parameters and CBF

Increment of ICP produced a fall in the regional blood flow of the cortical surface supplied by the left MCA, as shown in Fig 2. The correlation between TCD parameters and CBF was analyzed by linear regression (Fig 3). Although there was no significant linear correlation either between RI and CBF ($R^2 = .554$) or PI and CBF ($R^2 = .418$), using a logarithmic scale, CBF was statistically correlated with PI ($R^2 = .812$). This observation suggests that PI is a more indicative parameter of CBF than RI under conditions of intracranial hypertension. As shown in Fig 4, when the PI was >3.0 , percent CBF was $<20\%$, and when the PI was >4.0 , percent CBF was $<10\%$.

Electrophysiological Study

A typical course of ECoG changes under rapidly progressing intracranial hypertension is shown in Fig 2. A decrease in CBF caused by intracranial hypertension was detectable before conspicuous changes in the ECoG. Intracranial hypertension caused a suppression of electrocorticographic activity, which began at the SW stage of the flow pattern. The frequency of the ECoG had decreased markedly by the SF stage of the flow pattern. Finally, electroencephalographic standstill and dilatation of the pupils were observed at the NF stage of the flow pattern.

Discussion

Cerebral Microcirculation Under Marked Intracranial Hypertension

Under conditions of progressive intracranial hypertension, disturbances of CBF begin at the microcirculatory level and then extend to the larger vessels. Red blood cells begin to slough, and flow velocity through the veins and arteries slows down. If most of the capillaries are completely collapsed or obstructed, inefficient circulation is observed in the other blood vessels. With the sudden rise in ICP, blood flow is decreased markedly in both veins and arteries. The sloughing of red blood cells, intravascular agglutination and clotting, and microemboli formation occur in the later stages of cerebral compression. Finally the blood flow ceases almost entirely.⁹

Procedures to monitor ICP, such as intraventricular or epidural methods, are invasive and can cause serious complications. Preliminary reports on Doppler ultrasonography suggest that the Doppler spectrum can provide information related to ICP. Klingelhöer et al¹⁰ evaluated RI-ICP correlation in 13 comatose patients with various cerebral diseases and suggested an intimate relationship between ICP and the Doppler parameters. Chan et al¹¹ reported in their clinical study that PI was more closely correlated with CPP than with ICP or blood pressure. If CPP decreased to <70 mm Hg, a progressive increase in PI was observed. Homburg et al¹² observed a positive exponential correlation between PI and ICP in patients with head injuries. Hassler et al¹³ described characteristic flow patterns recorded by TCD in patients with markedly increased ICP. These reports, however, have not shown a direct correlation between TCD parameters and CBF.

Researchers^{14,15} who have attempted to apply Doppler instruments in experimental studies of brain death have met with a common problem: Doppler ultrasonographic procedures require appropriately sized blood vessels and an appropriate insonation angle. TCD ultrasonographic measurement of MCA flow in animal models has been an unreliable procedure because of the presence of the temporal bone, which prevents confirmation of vessel size and insonation angle. These technical difficulties have precluded the study of correlations between TCD parameters and CBF. A transorbital approach and the use of microvascular Doppler apparatus in the present study permitted circumvention of these problems. The MCA could be easily identified through the dura, and 20-MHz pulsed-wave microvascular Doppler sonography offered a smaller sample volume and permitted the proper insonation angle.

Flow Pattern and CBF

In this study, progressive intracranial hypertension brought about increased

pulsatility by reducing the flow velocity in the diastolic phase more rapidly than in the systolic phase. This phenomenon implies a loss of intracranial compliance under conditions of raised ICP.

Progressive changes in the TCD waveform provoked by increases in ICP were classified into four characteristic flow patterns. These changes in the flow pattern closely paralleled the changes in intracranial circulation that ultimately lead to arrest. Ungersböck et al¹⁶ suggested that TCD parameters were correlated with the percent change in red blood cell velocity in the microcirculation. We studied the percent change in cortical microcirculation by means of a laser-Doppler flowmeter that allowed continuous measurement of CBF without invading or damaging the tissue and permitted an analysis of the cortical microcirculation in terms of absolute values.

The critical level of CBF for cerebral electrophysiological failure is said to be approximately 30% (15 to 18 mL · 100g⁻¹ · min⁻¹) of the normal range, and that for cell membrane failure is about 20% (10 to 12 mL · 100g⁻¹ · min⁻¹).¹⁷ In our study, the percent CBF for the SF stage was approximately 30%. The frequency of the ECoG at the SF stage of the flow pattern was conspicuously low. Percent CBF values <10% provoked the SS pattern and the NF stage of the flow pattern. Therefore, a persistent SS stage could cause cell membrane failure. Moreover, these observations provide the strongest evidence yet that the ECoG is flattened during the NF stage of the flow pattern. These results suggest that the characteristic TCD flow waves, SS and NF, can be used as indexes of cortical CBF associated with brain death. These results corroborate those of other studies.^{18,19}

Ungersböck et al¹⁶ reported that RI was inversely related to CPP and that PI had an inverse exponential correlation with CPP. In this study, we analyzed the relationship between TCD parameters, including RI and PI, and microcirculatory flow. Logarithmic CBF values were correlated with RI and PI (Fig 3). This observation suggests that PI is more indicative of impaired CBF than RI and that PI could be used clinically to assess impairment in CBF due to intracranial hypertension. As shown in Fig 3, CBF was <8 mL · 100g⁻¹ · min⁻¹ when the PI value was >2.0, whereas CBF was <3 mL · 100g⁻¹ · min⁻¹ when the PI value was >4.0. A percent CBF value of <20% was correlated with a PI value of >4.0 (Fig 4). PI is one of the most reliable parameters to indicate the CBF level that can provoke irreversible neuronal damage.

In this study, oscillating flow (to-and-fro pattern)²⁰ was not observed in the later stages of intracranial hypertension. It is speculated that lack of the oscillating phase is related to differences in vascular anatomy and size between humans and cats,

which have an abundant blood supply from the external carotid rete²¹ and which have very small main vessels. In addition, this focal compression model causes a disproportionate increase in local ICP, and the resistance of the MCA can overcome that of collateral flow. Reflux flow is then directed to the external carotid rete via a rich collateral pathway and does not return to the MCA. To prove this hypothesis, warm saline was infused into the subdural space in cats to increase ICP diffusely and proportionally. Following this procedure, the oscillating pattern was observed at the same stage as the systolic spikes (Fig 5). With diffuse increases in ICP, both the MCA and collateral pathway are compressed evenly, and the reflux flow is spread into not only the external carotid rete but also the MCA. The oscillating pattern is suspected to indicate the same changes as the SS pattern, and both the oscillating pattern and the SS pattern as observed by TCD examination are accurate markers in the diagnosis of brain death.

Conclusion

With increases in ICP, the sonogram for the MCA demonstrated characteristic flow patterns that appeared in the following order: normal flow, sharp wave, systolic flow, systolic spike, and no flow. Each flow pattern was significantly correlated with ICP, CPP, and CBF. The flow pattern and PI may be useful indexes of CBF failure under conditions of intracranial hypertension. We believe that TCD is a useful adjunct for the detection of critical cerebral circulation provoking irreversible neuronal damage and brain death.

Acknowledgment

This study was supported by a grant-in-aid for scientific research on priority area from the Ministry of Education, Science, and Culture "Biomechanics" (Japan).

References

1. Newell DW, Grady MS, Sirotta P, Winn HR. Evaluation of brain death using transcranial Doppler. *Neurosurgery*. 1989;24:509-513.
2. Powers AD, Graeber MC, Smith RR. Transcranial Doppler ultrasonography in the determination of brain death. *Neurosurgery*. 1989;24:884-889.
3. Petty GW, Mohr JP, Pedley TA, Tatemichi TK, Lennihan L, Duterte DI, Sacco RL. The role of transcranial Doppler in confirming brain death: sensitivity, specificity, and suggestions for performance and interpretation. *Neurology*. 1990;40:300-303.
4. Langfitt TW, Weinstein JD, Kassell NF, Simeone FA. Transmission of increased intracranial pressure. I. *J Neurosurg*. 1964;21:989-997.
5. Hudgins WR, Garcia JH. Transorbital approach to the middle cerebral artery of the squirrel monkey: a technique for experimental cerebral infarction applicable to ultrastructural studies.

- Stroke*. 1970;1:107-111.
6. Yamasaki T, Moritake K, Takaya M, Kagawa T, Nagai H, Akiyama Y, Kawahara M. Intraoperative use of Doppler ultrasound and endoscopic monitoring in the stereotactic biopsy of malignant brain tumors. *J Neurosurg*. 1994;80:570-574.
 7. Gosling RG, King DH. Arterial assessment by Doppler shift ultrasound. *Proc R Soc Med*. 1974;67:447-449.
 8. Pourcelot L. Diagnostic ultrasound for cerebral vascular disease. In: Donald I, Levis S, eds. *Present and Future of Diagnostic Ultrasound*. Rotterdam, Netherlands: Kooyker; 1976:141-147.
 9. Hekmatpanah J. Cerebral circulation and perfusion in experimental increased intracranial pressure. *J Neurosurg*. 1970;32:21-29.
 10. Klingelhöer J, Sander D, Holzgraefe M, Bischoff C, Conrad B. Cerebral vasospasm evaluated by transcranial Doppler ultrasonography at different intracranial pressures. *J Neurosurg*. 1991;75:752-758.
 11. Chan KH, Miller JD, Dearden NM, Andrews PJD, Midgley S. The effect of changes in cerebral perfusion pressure upon middle cerebral artery blood flow velocity and jugular bulb venous oxygen saturation after severe brain injury. *J Neurosurg*. 1992;77:55-61.
 12. Homburg AM, Jakobsen M, Enevoldsen E. Transcranial Doppler recordings in raised intracranial pressure. *Acta Neurol Scand*. 1993;87:488-493.
 13. Hassler W, Steinmetz H, Pirschel J. Transcranial Doppler study of intracranial circulatory arrest. *J Neurosurg*. 1989;71:195-201.
 14. Barzó P, Dóczy T, Csete K, Buza Z, Bodosi M. Measurements of regional cerebral blood flow and blood flow velocity in experimental intracranial hypertension: infusion via the cisterna magna in rabbits. *Neurosurgery*. 1991;28:821-825.
 15. Arita K, Uozumi T, Kuwabara S, Oki S, Nakahara T, Kohno H, Muttaqin Z. Transcranial Doppler sonography in intracranial hypertension and brain death: its usefulness and pit falls. *Neurosonology* 1991;4:60-65.
 16. Ungersböck K, Tenckhoff D, Med C, Heimann A, Wagner W, Kempfski OS. Transcranial Doppler and cortical microcirculation at increased intracranial pressure and during the Cushing response: an experimental study on rabbits. *Neurosurgery*. 1995;36:147-157.
 17. Astrup J. Energy-requiring cell functions in the ischemic brain: their critical supply and possible inhibition in protective therapy. *J Neurosurg*. 1982;56:482-497.
 18. Takaya M, Moritake K, Fukuma A, Kagawa T, Nagai H. An experimental study on the transcranial Doppler ultrasonography in raised intracranial pressure. In: Oka M, von Reutern GM, Furuhashi H, Kodaira K, eds. *Recent Advances in Neurosonology*, Hiroshima, Japan: Elsevier Science Publishers BV; 1992:233-237.
 19. Shiogai T, Sato E, Tokitsu M, Hara M, Takeuchi K. Transcranial Doppler monitoring in severe brain damage: relationships between intracranial haemodynamics, brain dysfunction and outcome. *Neurol Res*. 1990;12:205-213.
 20. Yoneda S, Nishimoto A, Nukada T, Kuriyama Y, Katsurada K, Abe H. To-and-fro movement and external escape of carotid arterial blood in brain death cases: a Doppler ultrasonic study. *Stroke* 1974;5:707-713.
 21. Kamijyo Y, Garcia J. Carotid arterial supply of the feline brain. *Stroke* 1975;6:361-369.

Table. MFV indicates mean flow velocity. Serial changes in the time-averaged MFV, the RI, PI, ICP, CPP, CBF, and percent CBF at every stage of the Doppler flow pattern are shown. Mean \pm SD values were significantly different by Spearman's rank correlation test. With increases in ICP, the RI and PI increased, whereas MFV and CPP decreased. It is interesting to note that CBF and percent CBF declined during the stage characterized by the SS pattern.

Flow Patterns and Mean Values of Some Variables

Variable	Flow pattern, Mean \pm SD				
	Normal	SW	SF	SS	NF
MFV, cm/s	52.4 \pm 14.8	34.0 \pm 7.1	16.5 \pm 7.6	4.8 \pm 1.8	0.0 \pm 0.0
RI	0.5 \pm 0.1	0.6 \pm 0.1	1.0 \pm 0.0	1.0 \pm 0.0	1.0 \pm 0.0
PI	0.7 \pm 0.2	1.2 \pm 0.4	2.4 \pm 0.4	5.3 \pm 1.7	9.7 \pm 0.9
ICP, mm Hg	3.0 \pm 2.9	17.7 \pm 9.5	44.1 \pm 9.7	64.7 \pm 14.8	82.6 \pm 7.9
CPP, mm Hg	82.4 \pm 14.3	59.9 \pm 19.4	29.2 \pm 18.8	3.2 \pm 21.3	-21.3 \pm 14.8
CBF, mL \cdot 100g ⁻¹ \cdot min ⁻¹	15.5 \pm 7.7	9.3 \pm 3.9	4.7 \pm 1.6	1.2 \pm 0.5	0.6 \pm 0.2
Percent CBF	92.6 \pm 8.4	61.7 \pm 15.9	29.0 \pm 13.0	4.4 \pm 4.0	0.2 \pm 0.3

Selected Abbreviations and Acronyms

- CBF = cerebral blood flow
- CPP = cerebral perfusion pressure
- ECoG = cortical electroencephalography
- ICP = intracranial pressure
- MCA = middle cerebral artery
- NF = no flow
- PI = pulsatility index
- RI = resistance index
- SF = systolic flow
- SS = systolic spike
- SW = sharp wave
- TCD = transcranial Doppler ultrasonography

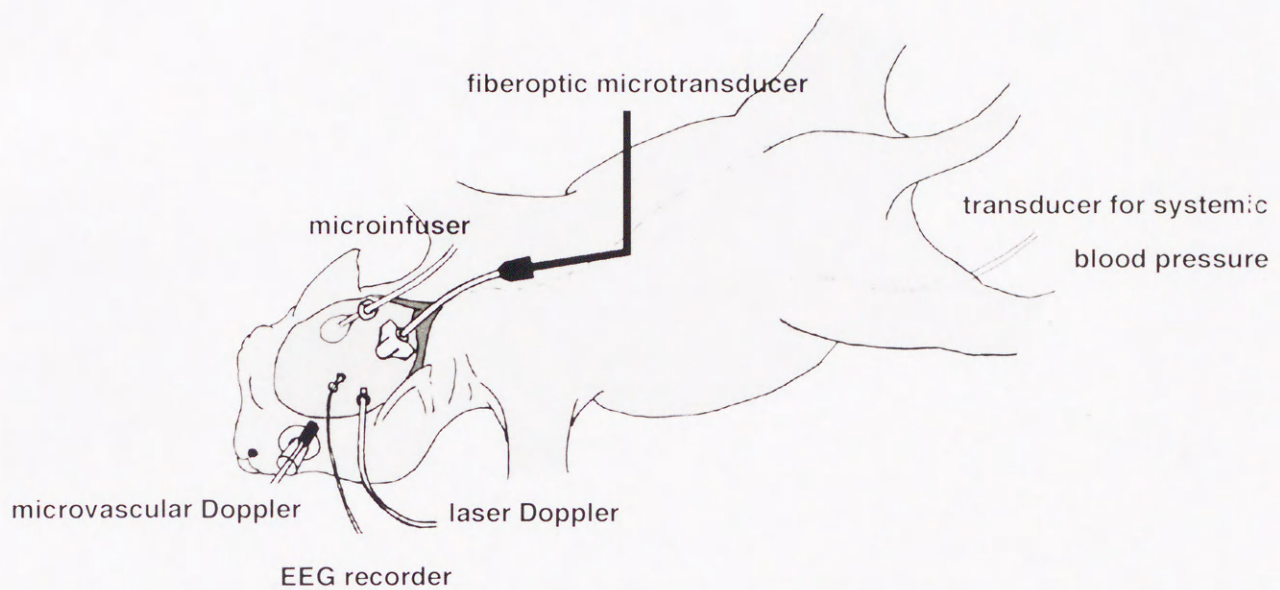


Fig 1. Schematic drawing of the experiment illustrates the supratentorial epidural balloon model in cats. Systemic arterial blood pressure was measured by transfemoral catheterization. ICP was measured with a fiberoptic microtransducer inserted into the epidural space. CBF was measured by laser-Doppler flowmetry through a burr hole placed over the left ectosylvian gyrus. Electroencephalography of the left ectosylvian gyrus of cats was recorded from an epidural electrode placed near the laser-Doppler flowmetry probe. The epidural balloon was inflated at an injection rate of 0.047 mL/min using a microinfuser. The Doppler sonogram was measured transorbitally by 20-MHz pulsed-wave microvascular Doppler ultrasonography. The MCA was identified through the dura by a transorbital approach.

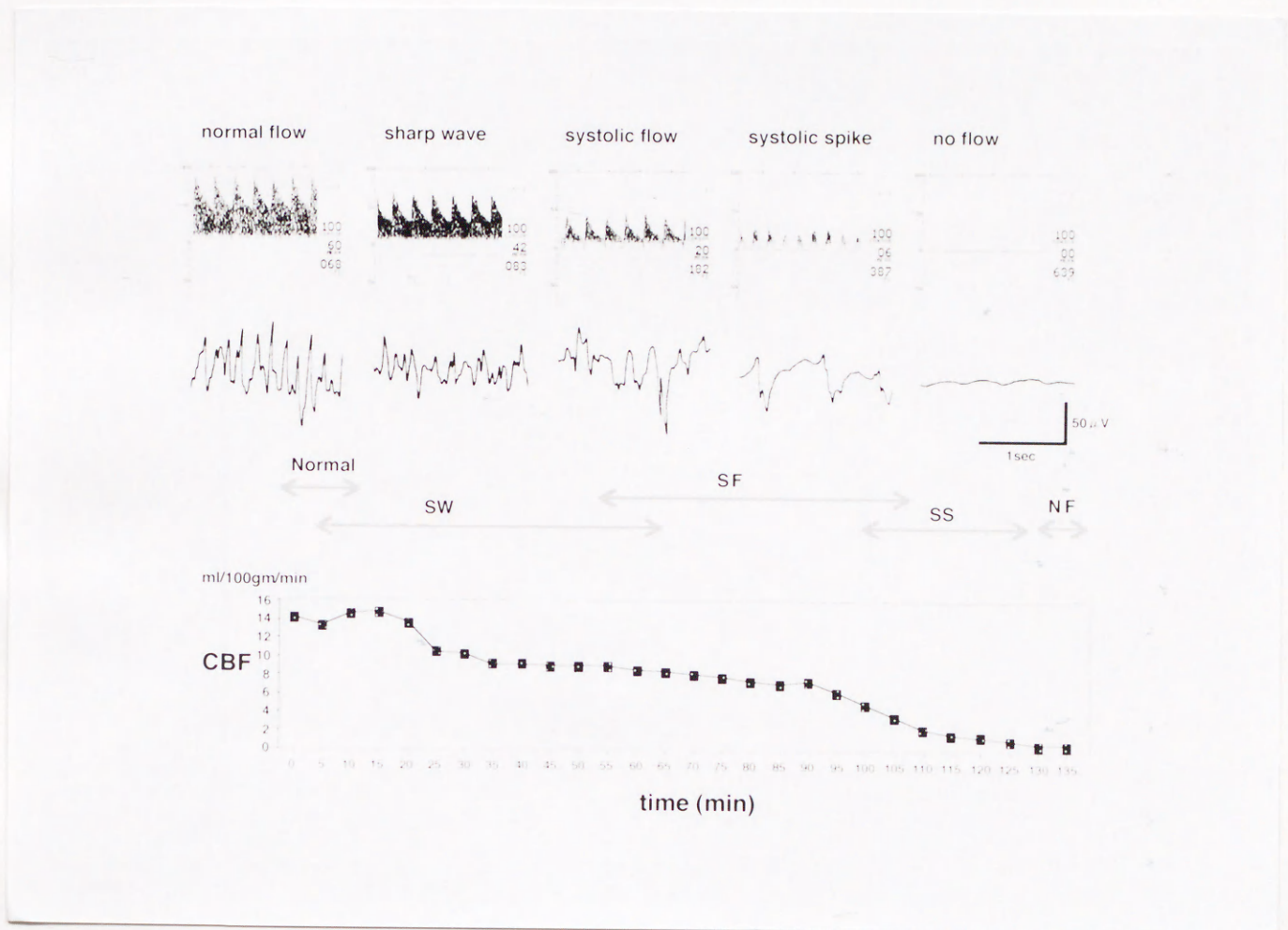


Fig 2. Sequential changes in flow pattern, ECoG, and CBF. Relationships between the Doppler flow pattern, ECoG, and CBF were obtained in our model. Five flow patterns were observed with increases in ICP and appeared in the following sequence: normal, SW, SF, SS, and NF. Suppression of electroencephalographic activity and decline in CBF were detected as with the increased ICP.



Figure 1. Left: Plot of Y vs X

Figure 2. Right: Plot of Y vs X

Figure 3. Plot of Y vs X

The plot shows a clear upward trend, indicating a positive correlation between X and Y. The data points are scattered around a fitted line, suggesting some variability in the data. The plot is titled 'Figure 3. Plot of Y vs X'.

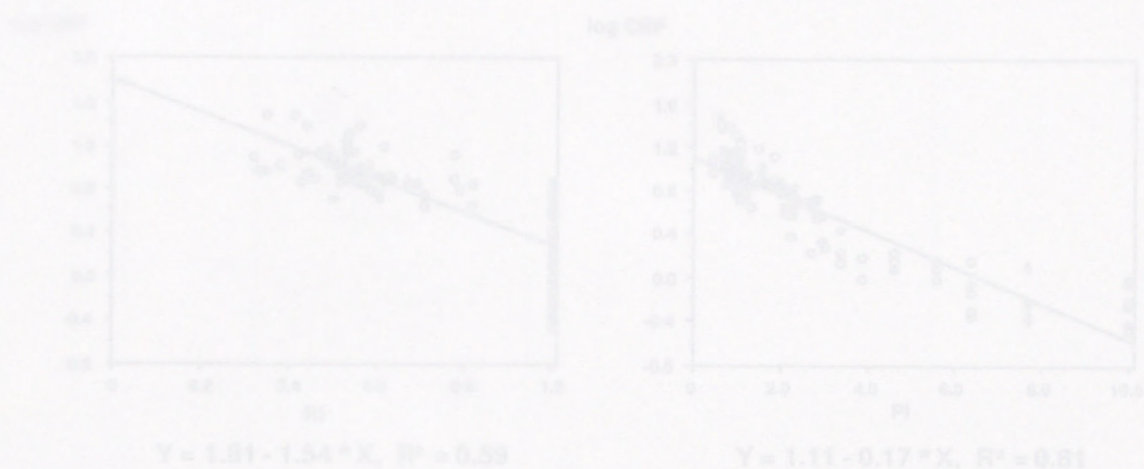


Fig 3. Relationship between CBF and RI and between CBF and PI. The left scatterplot shows the correlation between logarithmic CBF and RI. The right scatterplot shows the relationship between logarithmic CBF and PI. PI was statistically correlated with logarithmic CBF.

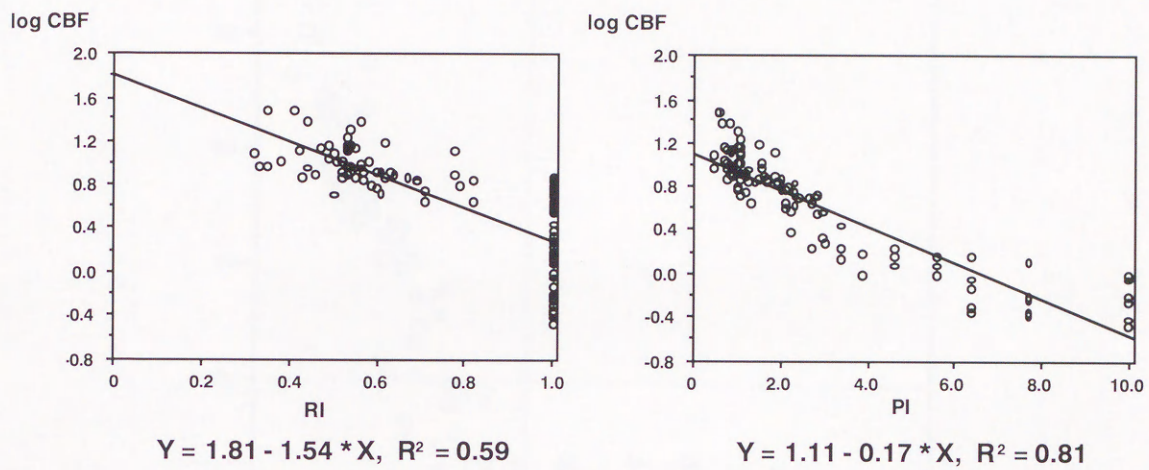


Fig 3. Relationship between CBF and RI and between CBF and PI. The left scatterplot shows the correlation between logarithmic CBF and RI. The right scatterplot shows the relationship between logarithmic CBF and PI. PI was statistically correlated with logarithmic CBF.

percent CBF

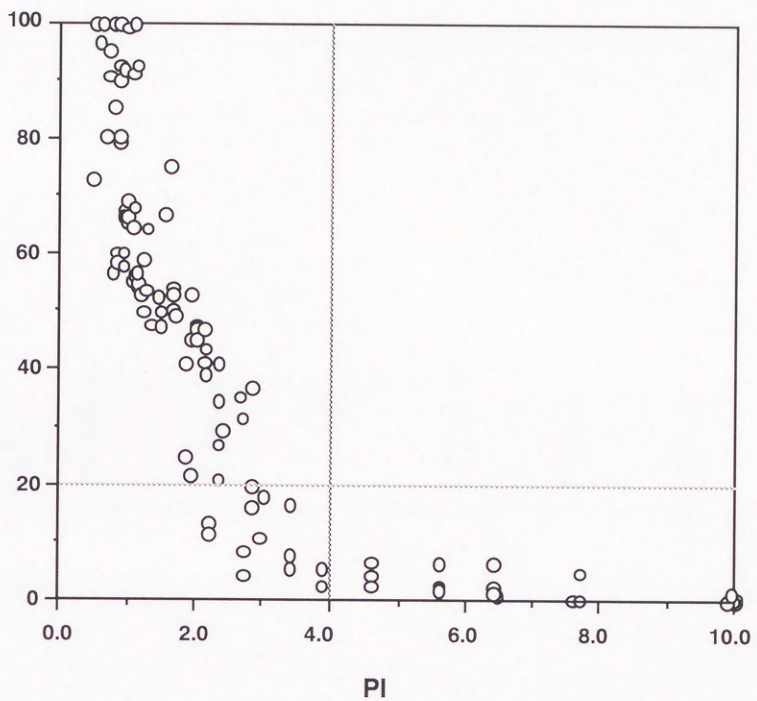


Fig 4. Relationship between percent CBF and PI. PI was negatively correlated with percent CBF. The percent CBF was always <20% whenever PI was >4.0.



Fig 5. Oscillating pattern recorded in a subject with a low ICP. The oscillating pattern was observed at the same stage in the control model as the elevated ICP model in which ICP was elevated diffusely and progressively. The presence of the oscillating pattern may be related to the reflux of the ICP & CSF waves with occasional increases in ICP.

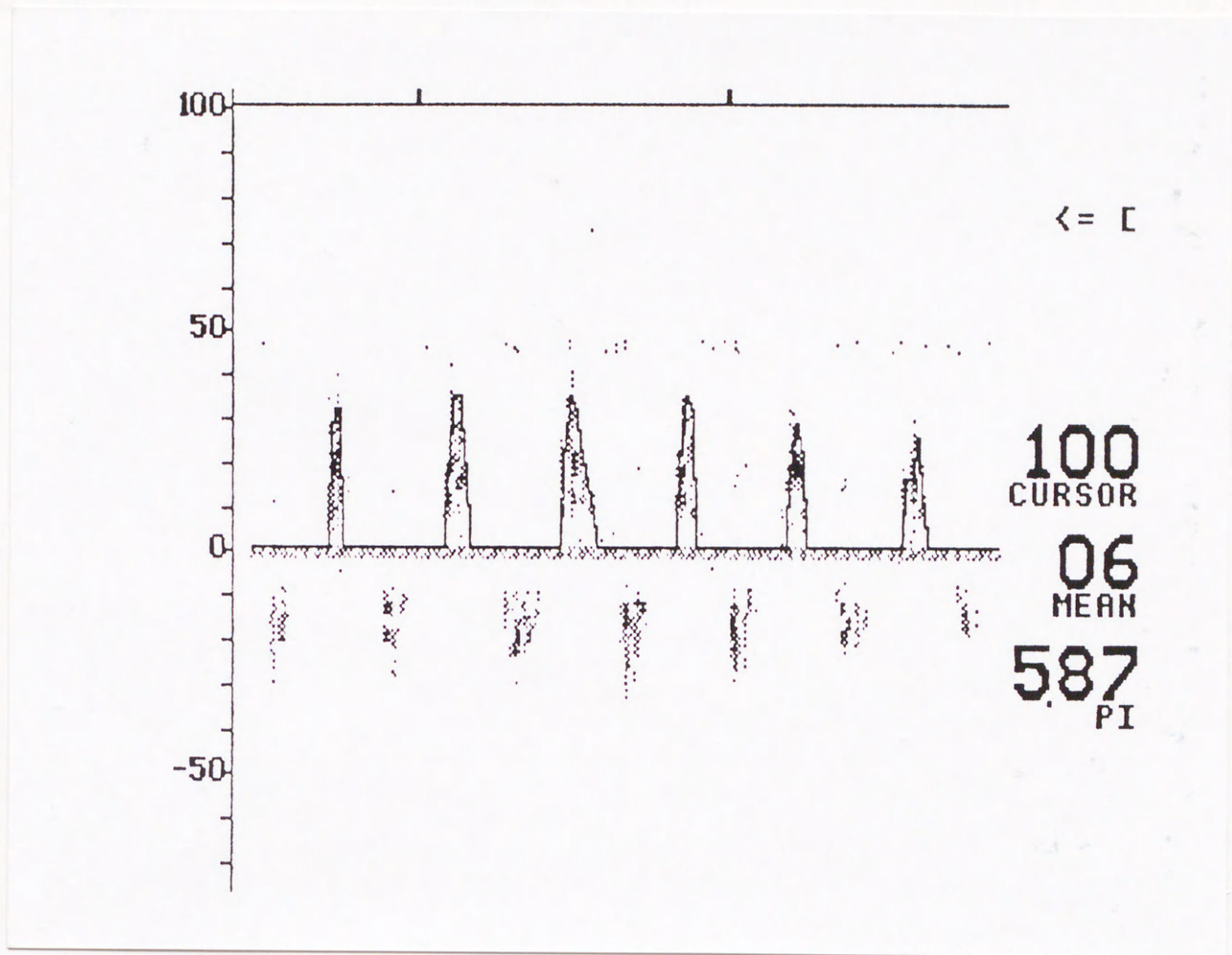
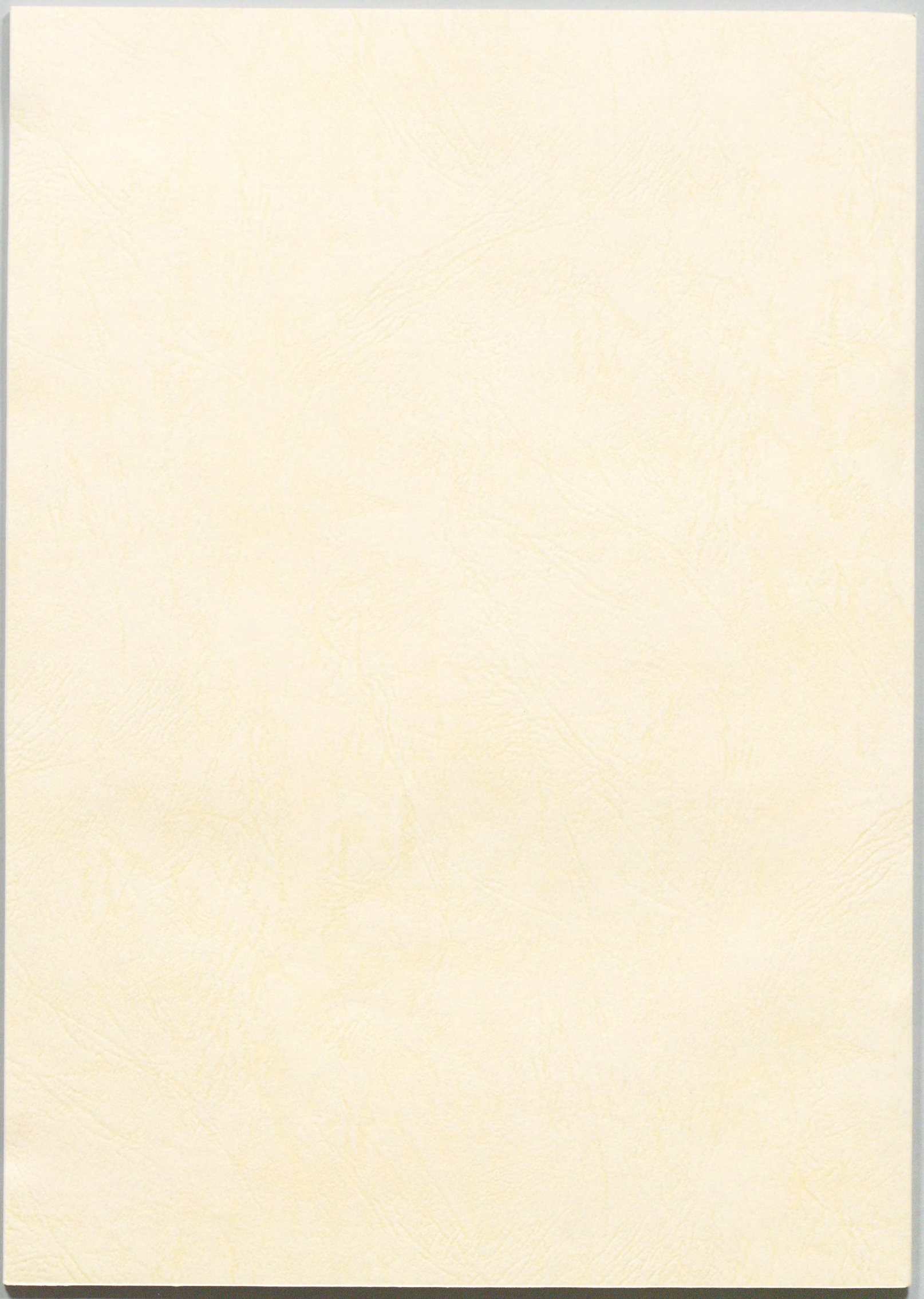


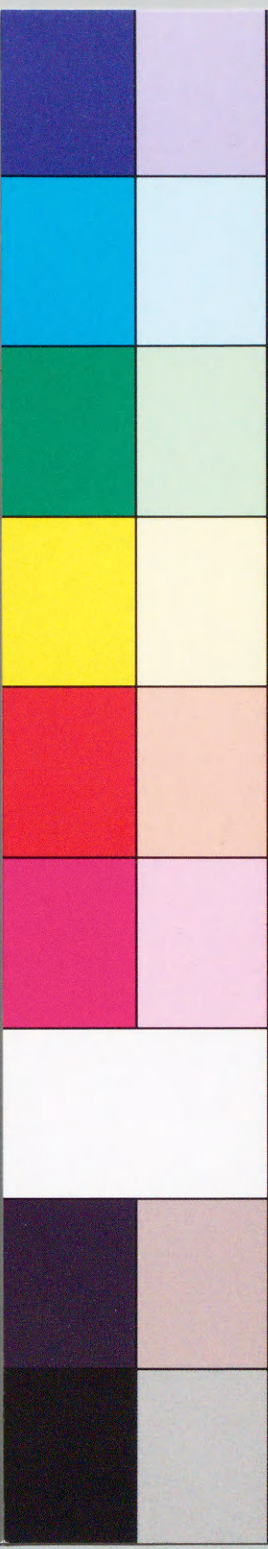
Fig 5. Oscillating pattern recorded in subdural infusion model. The oscillating pattern was observed at the same stage as the systolic spikes in the subdural infusion model in which ICP was elevated diffusely and proportionally. The generation of the oscillating pattern may be related to the reflux of the MCA blood flow with proportional incremental increases in ICP.



Inches 1 2 3 4 5 6 7 8
cm 1 2 3 4 5 6 7 8 9 10 11 12 13 14 15 16 17 18 19

Kodak Color Control Patches

Blue Cyan Green Yellow Red Magenta White 3/Color Black



Kodak Gray Scale

A 1 2 3 4 5 6 M 8 9 10 11 12 13 14 15 B 17 18 19



© Kodak, 2007 TM: Kodak